Acta Cryst E CRYSTALLOGRAPHIC COMMUNICATIONS

ISSN 2056-9890

[μ_2-*trans*-1,2-Bis(pyridin-4-yl)ethene-κ^2N:N']-bis{[1,2-bis(pyridin-4-yl)ethene-κN]bis[*N*-(2-hydroxyethyl)-*N*-isopropyldithiocarbamato-κ^2S,S']-cadmium} acetonitrile tetrasolvate: crystal structure and Hirshfeld surface analysis

Mukesh M. Jotani,[a]‡ Pavel Poplaukhin,[b] Hadi D. Arman[c] and Edward R. T. Tiekink[d]*

[a]Department of Physics, Bhavan's Sheth R. A. College of Science, Ahmedabad, Gujarat 380 001, India, [b]Chemical Abstracts Service, 2540 Olentangy River Rd, Columbus, Ohio 43202, USA, [c]Department of Chemistry, The University of Texas at San Antonio, One UTSA Circle, San Antonio, Texas 78249-0698, USA, and [d]Centre for Crystalline Materials, Faculty of Science and Technology, Sunway University, 47500 Bandar Sunway, Selangor Darul Ehsan, Malaysia. *Correspondence e-mail: edwardt@sunway.edu.my

Received 28 June 2016
Accepted 4 July 2016

Edited by W. T. A. Harrison, University of Aberdeen, Scotland

‡ Additional correspondence author, e-mail: mmjotani@rediffmail.com.

Keywords: crystal structure; dithiocarbamate; 1,2-bis(pyridin-4-yl)ethene; interpenetration; hydrogen bonding; Hirshfeld surface analysis.

CCDC reference: 1489732

Supporting information: this article has supporting information at journals.iucr.org/e

The asymmetric unit of the title compound, $[Cd_2(C_{12}H_{10}N_2)_3(C_6H_{12}NOS_2)_4]\cdot 4C_2H_3N$, comprises a Cd^{II} atom, two dithiocarbamate (dtc) anions, one and a half *trans*-1,2-dipyridin-4-ylethylene (bpe) molecules and two acetonitrile solvent molecules. The full binuclear complex is generated by the application of a centre of inversion. The dtc ligands are chelating, one bpe molecule coordinates in a monodentate mode while the other is bidentate bridging. The resulting *cis*-N_2S_4 coordination geometry is based on an octahedron. Supramolecular layers, sustained by hydroxy-O—H···O(hydroxy) and hydroxy-O—H···N(bpe) hydrogen bonding, interpenetrate to form a three-dimensional architecture; voids in this arrangement are occupied by the acetonitrile solvent molecules. Additional intermolecular interactions falling within the specified framework have been analysed by Hirshfeld surface analysis, including π–π interactions.

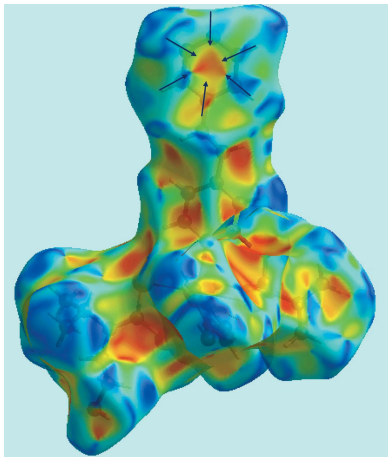

OPEN ACCESS

1. Chemical context

The recent disclosure of one-dimensional, supramolecular isomers of $\{Cd[S_2CN(iPr)CH_2CH_2OH]_2\}_n$ notwithstanding (Tan *et al.*, 2013, 2016), the overwhelming majority of binary bis(dialkyldithiocarbamato) compounds of cadmium are usually binuclear with a coordination number of five owing to the presence of equal numbers of chelating and μ_2-tridentate ligands, *i.e.* are of general formula $[Cd(S_2CNR_2)_2]_2$ (Tiekink, 2003; Tan *et al.*, 2016). However, the dimeric and polymeric aggregates are readily broken down in the presence of bases such as monodentate pyridine, *e.g.* $\{Cd[S_2CN(CH_2C(H)Me_2)_2]_2(pyridine)\}$ (Rodina *et al.*, 2011) and bidentate 2,2′-bipyridine, *e.g.* $[Cd(S_2CN(Me)iPr)_2(2,2'\text{-bipyridine})]$ (Wahab *et al.*, 2011). Bridging N-donors lead to a greater variety of structures such as the zero-dimensional binuclear compound, $[Cd(S_2CNPr_2)_2(2\text{-pyridinealdazine})]_2$ (Poplaukhin & Tiekink, 2008) and supramolecular chains, *e.g.* $[Cd(S_2CNEt_2)_2(\mu_2\text{-}1,2\text{-bis(4-pyridyl)ethylene})]_n$ (Chai *et al.*, 2003). The addition of hydrogen-bonding functionality in the dithiocarbamate ligands has greatly enhanced the supramolecular chemistry landscape of related compounds. As a recent exemplar, the

formally monomeric compound {Cd[$S_2CN(iPr)CH_2CH_2OH]_2$}(piperazine) self-assembles into a two-dimensional array *via* hydroxy-O—H···O(hydroxy), hydroxy-O—H···N(terminal-piperazine) and coordinating piperazine-N—H···O(hydroxy) hydrogen bonds (Safbri *et al.*, 2016). As a continuation of investigations in this area, the crystal and molecular structure as well as Hirshfeld surface analysis of the title binuclear compound, {Cd[$S_2CN(iPr)CH_2CH_2OH]_2$[(4-NC_5H_4)C═C_6H_4N-4)]}$_2$[(4-NC_5H_4)C═C_6H_4N-4)]·4CH_3CN, (I), featuring both bidentate bridging and monodentate *trans*-1,2-dipyridin-4-ylethylene ligands is described herein.

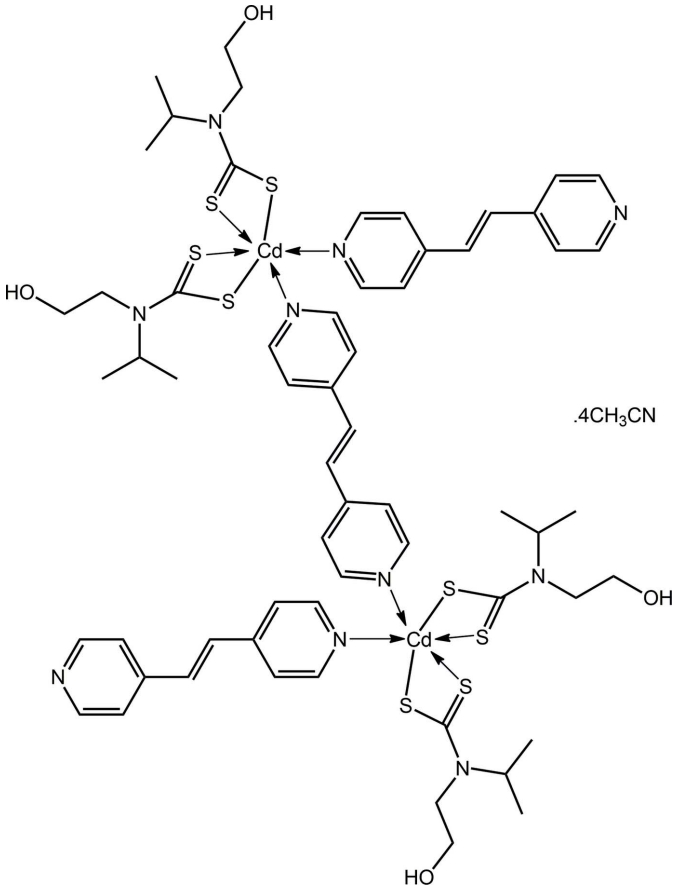

2. Structural commentary

The molecular structure of the binuclear title compound, {Cd[$S_2CN(iPr)CH_2CH_2OH]_2$[(4-NC_5H_4)C═C_6H_4N-4)]}$_2$[(4-NC_5H_4)C═C_6H_4N-4)]·4CH_3CN, (I), Fig. 1, is situated about a centre of inversion; two acetonitrile molecules of solvation complete the asymmetric unit. Each Cd^{II} atom is coordinated by two dithiocarbamate ligands and two nitrogen atoms, one derived from a monodentate *trans*-1,2-dipyridin-4-ylethylene (bispyridylethene; bpe) ligand and another from one end of a bidentate, bridging bpe ligand (located about a centre of inversion). The dithiocarbamate ligands coordinate with significant differences in their Cd—S bond lengths, Table 1. Thus, Δ(Cd—S) = d(Cd—S_{long}) − d(Cd—S_{short}) = 0.15 Å for the S1-dithiocarbamate ligand *cf.* 0.10 Å for the S3-ligand. Nevertheless, there is considerable delocalization of π-electron density in the CdS_2C chelate rings as evidenced by the equivalence of the associated C—S bond lengths, Table 1. The coordination geometry is based on an octahedron. In this description, the more tightly bound S1 and S3 atoms are *trans* [178.06 (3)°] and the less tightly bound sulfur atoms are *trans* to nitrogen atoms, Table 1, implying the nitrogen donors are *cis*. The distortions from the ideal geometry are readily related to the restricted bite angles of the chelating ligands, Table 1. Both bpe ligands exhibit twists as seen in the values of

Table 1
Selected geometric parameters (Å, °).

Cd—S1	2.6019 (8)	Cd—N4	2.454 (3)
Cd—S2	2.7457 (8)	C1—S1	1.726 (3)
Cd—S3	2.6043 (8)	C1—S2	1.717 (3)
Cd—S4	2.6967 (8)	C7—S3	1.721 (3)
Cd—N3	2.439 (3)	C7—S4	1.727 (3)
S1—Cd—S2	67.31 (2)	S2—Cd—N4	152.04 (6)
S1—Cd—S3	178.06 (3)	S3—Cd—S4	68.00 (2)
S1—Cd—S4	112.08 (3)	S3—Cd—N3	86.63 (7)
S1—Cd—N3	93.39 (7)	S3—Cd—N4	95.94 (6)
S1—Cd—N4	85.98 (6)	S4—Cd—N3	154.39 (6)
S2—Cd—S3	110.75 (3)	S4—Cd—N4	97.72 (6)
S2—Cd—S4	99.85 (3)	N3—Cd—N4	80.87 (9)
S2—Cd—N3	92.19 (7)		

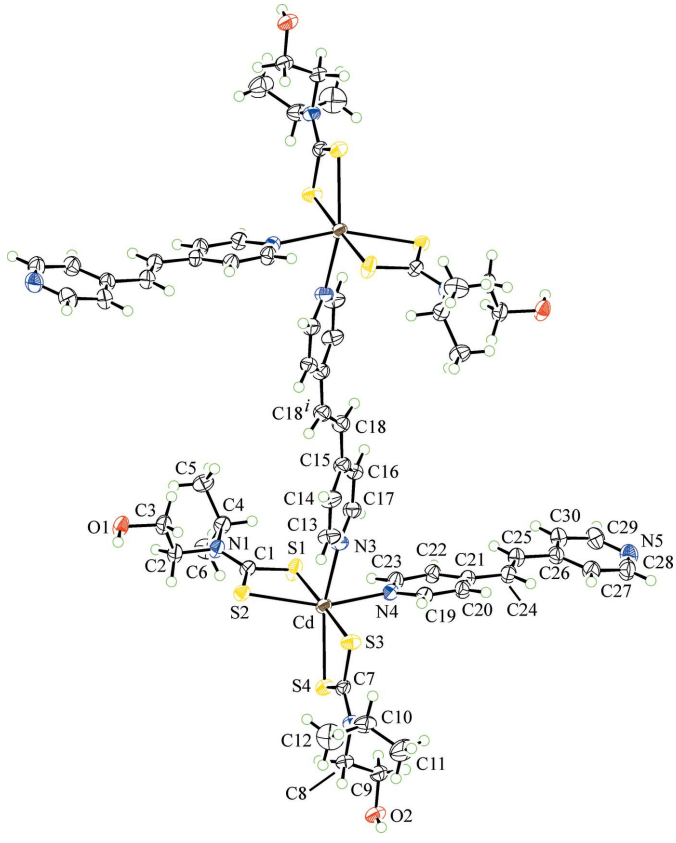

Figure 1
The molecular structure of the binuclear title compound in (I), showing the atom-labelling scheme and displacement ellipsoids at the 50% probability level. Unlabelled atoms are related by the symmetry operation (2 − x, −y, 1 − z.). The acetonitrile solvent molecules have been omitted for clarity.

Table 2
Hydrogen-bond geometry (Å, °).

D—H···A	D—H	H···A	D···A	D—H···A
O1—H1O···N5^{i}	0.83 (4)	1.82 (4)	2.655 (4)	177 (3)
O2—H2O···O1^{ii}	0.84 (3)	1.87 (3)	2.689 (3)	165 (5)
C25—H25···O2^{iii}	0.95	2.44	3.261 (4)	145
C28—H28···N7^{iv}	0.95	2.56	3.296 (7)	134

Symmetry codes: (i) $x-1, -y+\frac{1}{2}, z-\frac{1}{2}$; (ii) $x, y+1, z$; (iii) $-x+2, -y+1, -z+2$; (iv) $x+1, -y+\frac{3}{2}, z+\frac{1}{2}$.

the C14—C15—C18—C18^{i} and C22—C21—C24—C25 torsion angles of −12.2 (6) and 13.9 (5)° for the bi- and mono-dentate ligands, respectively; symmetry code: (i) $2-x, -y, 1-z$.

3. Supramolecular features

Geometric details of the significant intermolecular interactions are given in Table 2. In the packing, hydroxy-O—H···O(hydroxy) hydrogen bonding leads to supramolecular ladders as illustrated in Fig. 2*a*. These ladders are connected into layers parallel to (101) *via* hydroxy-O—H···N(bpe) hydrogen bonds where the nitrogen atom is derived from the monodentate bpe ligand. Additional ethene-C—H···O(hy-O(hydroxy) interactions are found within this framework, Table 2. As seen from Fig. 2*b*, this arrangement leads to rectangular channels with Cd···Cd separations, which approximate the edges, being 14 and 16 Å. Successive channels are largely occupied by other supramolecular layers, leading to a three-dimensional, concatenated architecture. The smaller voids defined by the interpenetrated structure are occupied by the solvent acetonitrile molecules, Fig. 2*c*. The N7-acetonitrile molecule is connected to the host framework by pyridyl-C—H···N(acetonitrile) interactions whereas the N6-acetonitrile molecule does not form significant interactions in accord with the criteria embodied in *PLATON* (Spek, 2009). This is reflected in the greater displacement ellipsoids for this molecule *cf.* with the N7-containing molecule. Further analysis of the molecular packing, *e.g.* pyridyl···pyridyl interactions, is given in the following Section.

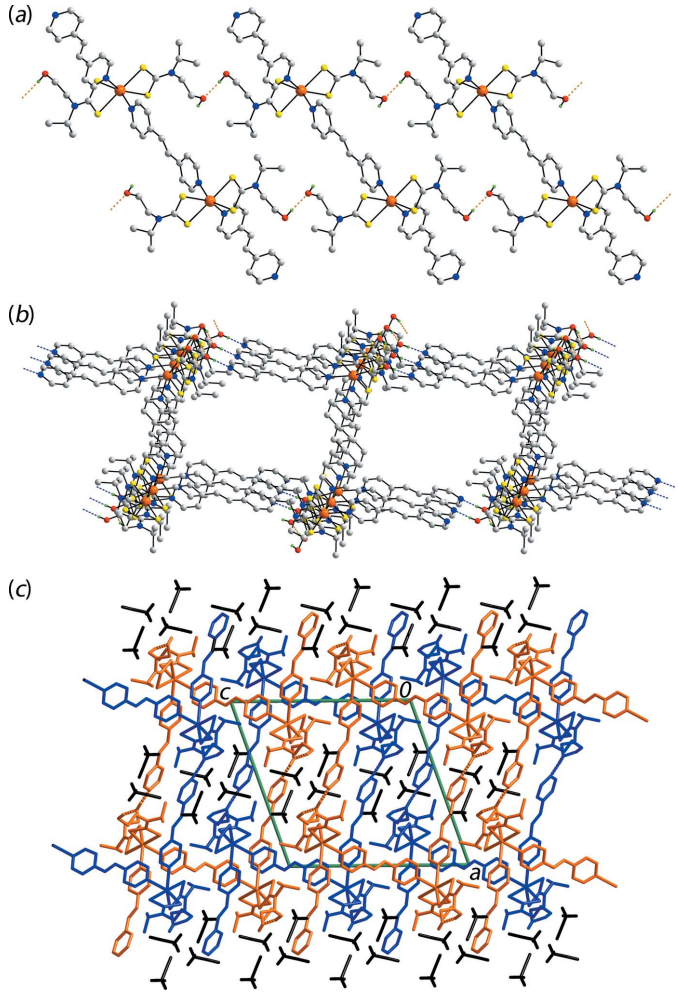

Figure 2
Molecular packing in (I): (*a*) view of the supramolecular ladder sustained by hydroxy-O—H···O(hydroxy) hydrogen bonds, shown as orange dashed lines, (*b*) two-dimensional framework whereby the layers in (*a*) are connected by hydroxy-O—H···N(bpe) hydrogen bonds, shown as blue dashed lines, (*c*) view of the unit-cell contents shown in projection down the *a* axis, highlighting the interpenetration of successive supramolecular layers, illustrated in orange and green, with solvent acetonitrile molecules shown in black.

4. Analysis of the Hirshfeld surfaces

Recent Hirshfeld surface analyses of zinc-triad hydroxyethyl-substituted dithiocarbamates has provided key insight into their molecular packing over and beyond hydrogen-bonding considerations. For example, the relatively unusual C—H···π(chelate) interactions (Tiekink & Zukerman-Schpector, 2011) observed in $[Hg(S_2CN(CH_2CH_2OH)_2]_n$ (Howie *et al.*, 2009), are clearly delineated in the Hirshfeld analysis of the molecular packing (Jotani *et al.*, 2016). In the present study, using *Crystal Explorer 3.1* (Wolff *et al.*, 2012), the Hirshfeld surfaces were mapped over d_{norm}, shape-index, curvedness and electrostatic potential for the asymmetric unit of (I). The electrostatic potentials were calculated using *TONTO* (Spackman *et al.*, 2008; Jayatilaka *et al.*, 2005) integrated into *Crystal Explorer*. Further, the electrostatic potentials were mapped on Hirshfeld surfaces using the STO–3G basis set at Hartree–Fock level of theory over a range ±0.13 au. The contact distances d_i and d_e from the Hirshfeld surface to the nearest atom inside and outside, respectively, enable the analysis of the intermolecular interactions through the mapping of d_{norm}. The combination of d_e and d_i in the form of two-dimensional fingerprint plots (McKinnon *et al.*, 2004) provides a summary of intermolecular contacts in the crystal.

Two views of Hirshfeld surfaces mapped over d_{norm} in the −0.2 to 1.8 Å range are shown in Fig. 3. The bright-red spots appearing near pyridyl-N5, hydroxy-O1 and hydrogen atoms H1*O* and H2*O* indicate their role as the respective donors and acceptors in the dominant O—H···O and O—H···N hydrogen bonds; they also appear as blue and red regions, respectively, corresponding to positive and negative electrostatic potentials on the Hirshfeld surface mapped over elec-

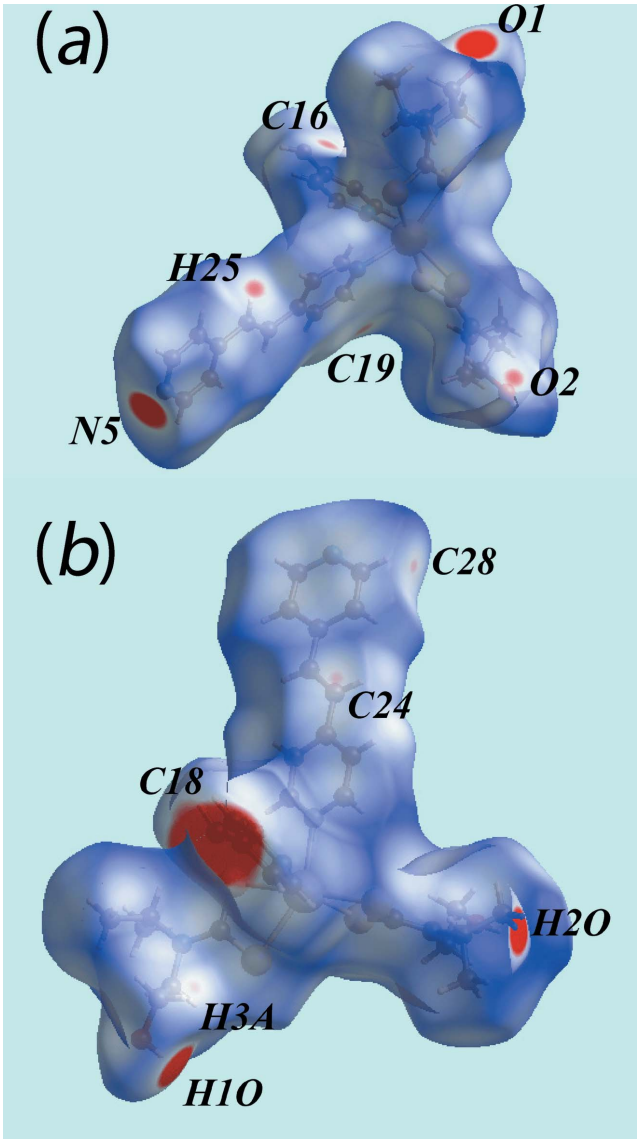

Figure 3
Two views of the Hirshfeld surface mapped over d_{norm}. The contact points (red) are labelled to indicate the atoms participating in the intermolecular interactions.

trostatic potential, Fig. 4. The light-red spots near ethene-H25, pyridyl-C28 and hydroxy-O2 in Fig. 3 and near acetonitrile-N7, Fig. 5*a*, indicate their involvement in the intermolecular ethene-C—H···O(hydroxy) and pyridyl-C—H···N(acetonitrile) interactions. The presence of short intermolecular C···C and C···H contacts, Table 3, is also evident from the light-red spots appearing near the pyridyl-C16, C19 and C24 and methylene-H3*A* atoms in Fig. 3. The C18—C18^{i} link of the bridging bpe ligand can be viewed as a bright-red region around the C18 atom in the d_{norm} mapped surface, Fig. 3, and as a light-blue region surrounded by a pair of light-red arcs on the surface mapped over electrostatic potential, Fig. 4*b*; this arises as it is the asymmetric unit that has been investigated not the entire binuclear molecule. With respect to the acetonitrile molecule the d_{norm} mapped surfaces show only the acetonitrile-N7 to be involved in a significant intermolecular

Table 3
Summary of short interatomic contacts (Å).

Contact	Distance	Symmetry
S1···H6*A*	2.98	$2-x, -y, 2-z$
S4···H18	2.97	$2-x, \frac{1}{2}+y, \frac{3}{2}-z$
O1···H11*C*	2.64	$x, -1+y, z$
O2···H30	2.66	$2-x, 1-y, 2-z$
C1···H20	2.83	$2-x, -\frac{1}{2}+y, \frac{3}{2}-z$
C3···H2*O*	2.69 (3)	$x, -1+y, z$
C24···H3*A*	2.72	$2-x, -\frac{1}{2}+y, \frac{3}{2}-z$
C28···H1*O*	2.83 (3)	$1+x, \frac{1}{2}-y, \frac{1}{2}+z$
C29···H1*O*	2.67 (4)	$1+x, \frac{1}{2}-y, 1+z$
C16···C19	3.245 (4)	$2-x, -\frac{1}{2}+y, \frac{3}{2}-z$
C16···C20	3.377 (5)	$2-x, -\frac{1}{2}+y, \frac{3}{2}-z$
H5*A*···H23	2.31	$2-x, -y, 2-z$

C—H···N interaction (Fig. 5*a*, Table 2), and both acetonitrile molecules had very similar Hirshfeld surfaces mapped over electrostatic potential to that for the N7-molecule illustrated in Fig. 5*b*.

The overall two-dimensional fingerprint plot, Fig. 6*a*, and those delineated into H···H, O···H/H···O, C···H/H···C, N···H/H···N, C···C and S···H/H···S contacts (McKinnon *et al.*, 2007) are illustrated in Fig. 6*b*-*g*, respectively; their relative

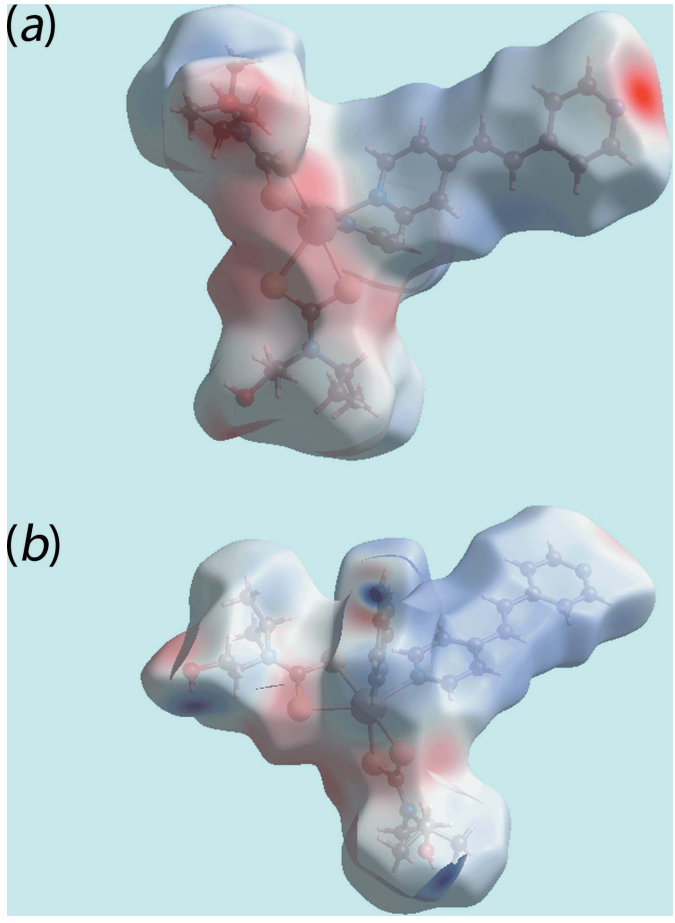

Figure 4
Two views of the Hirshfeld surface mapped over the electrostatic potential with positive and negative potential indicated in blue and red, respectively.

Table 4
Percentage contribution of the different intermolecular contacts to the Hirshfeld surface.

Contact	Contribution
H···H	51.9
O···H/H···O	6.0
C···H/H···C	15.9
N···H/H···N	10.6
C···C	3.1
S···H/H···S	10.3
C···S/S···C	0.8
N···S/S···N	0.7
C···N/N···C	0.7

contributions are summarized in Table 4. The H···H contacts make the greatest contribution to the Hirshfeld surface, *i.e.* 51.9% which is reflected in Fig. 6*b* as widely scattered points of high density due to the large hydrogen content of the molecule; the single peak at $d_e = d_i$ ~1.15 Å results from a short intermolecular H···H contact between the isopropyl-H5*A* and pyridyl-H23 atoms, Table 3. In the fingerprint plot delineated into O···H/H···O contacts, the 6.0% contribution to the Hirshfeld surface arises from the intermolecular O—H···O hydrogen bonding and is viewed as a pair of spikes with the tip at $d_e + d_i$ ~1.8 Å in Fig. 6*c*. The intermolecular C—H···O interactions and short O···H/H···O contacts, listed in Table 3, are masked by the strong O—H···O hydrogen bonding in this plot.

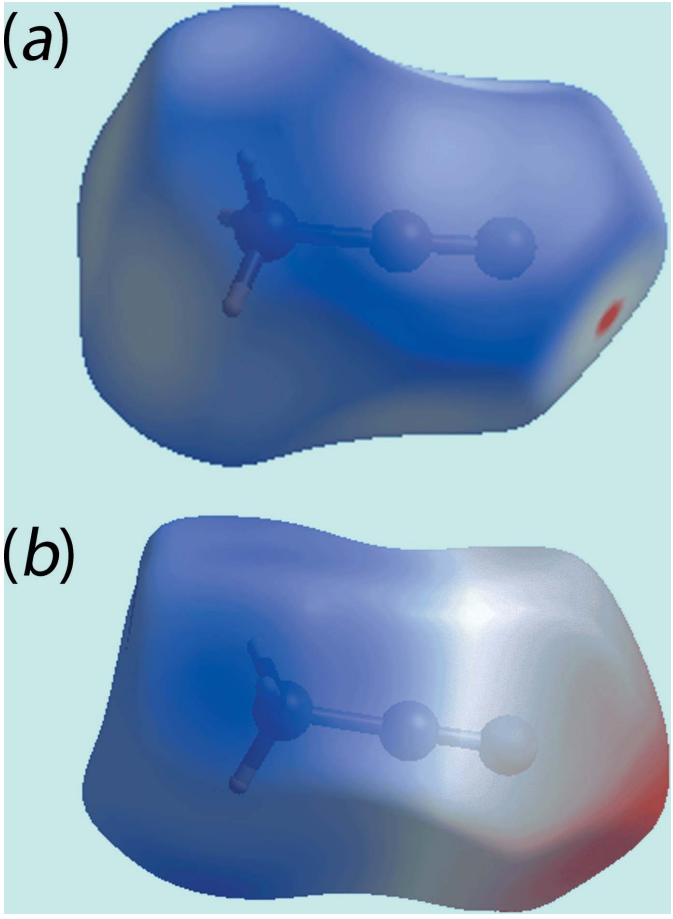

Figure 5
A view of the (*a*) Hirshfeld surface mapped over d_{norm} and (*b*) Hirshfeld surface mapped over the electrostatic potential with positive and negative potential indicated in blue and red, respectively, for the N7-acetonitrile molecule.

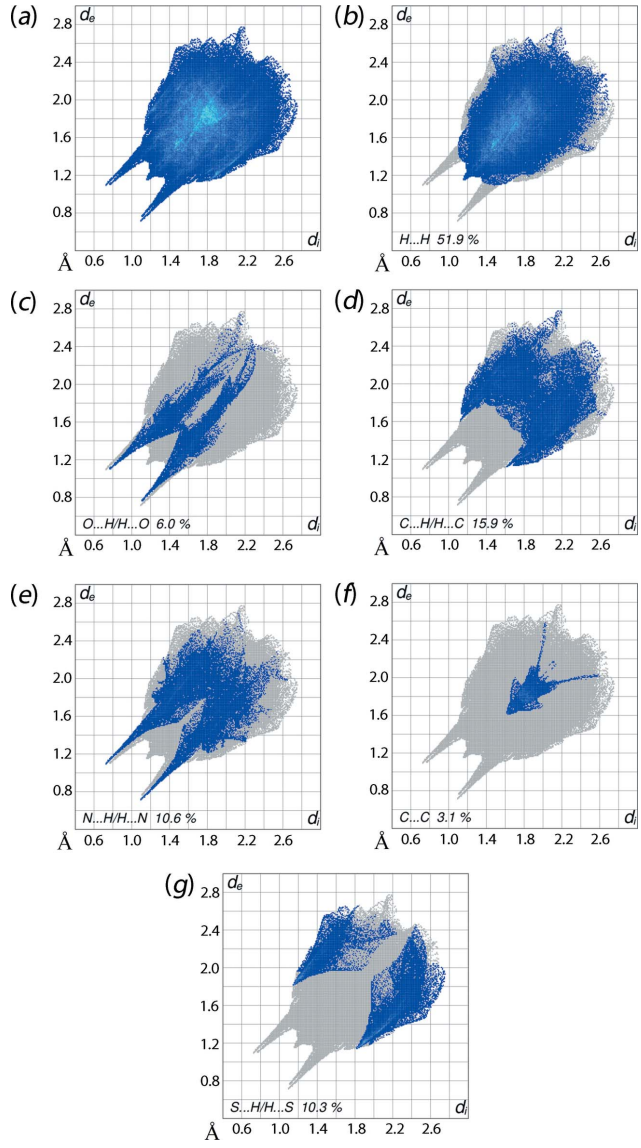

Figure 6
Two-dimensional fingerprint plots: (*a*) overall, and delineated into contributions from different contacts: (*b*) H···H, (*c*) O···H/H···O, (*d*) C···H/H···C, (*e*) N···H/H···N, (*f*) C···C and (*g*) S···H/H···S.

In the absence of C—H···π interactions in the crystal, the pair of characteristic wings resulting in the fingerprint plot delineated into C···H/H···C contacts with 15.9% contribution to the Hirshfeld surface, Fig. 6*d*, and the pair of thin edges at $d_e + d_i$ ~2.7 Å result from short interatomic C···H/H···C contacts, Table 3. A pair of spikes at $d_e + d_i$ ~1.8 Å correspond to N···H/H···N contacts, Fig. 6*e*, confirm the presence of intermolecular O—H···N and C—H···N interactions. The C···C contacts assigned to short interatomic C16···C19 and C16···C20 contacts listed in Table 3 and π–π stacking inter-

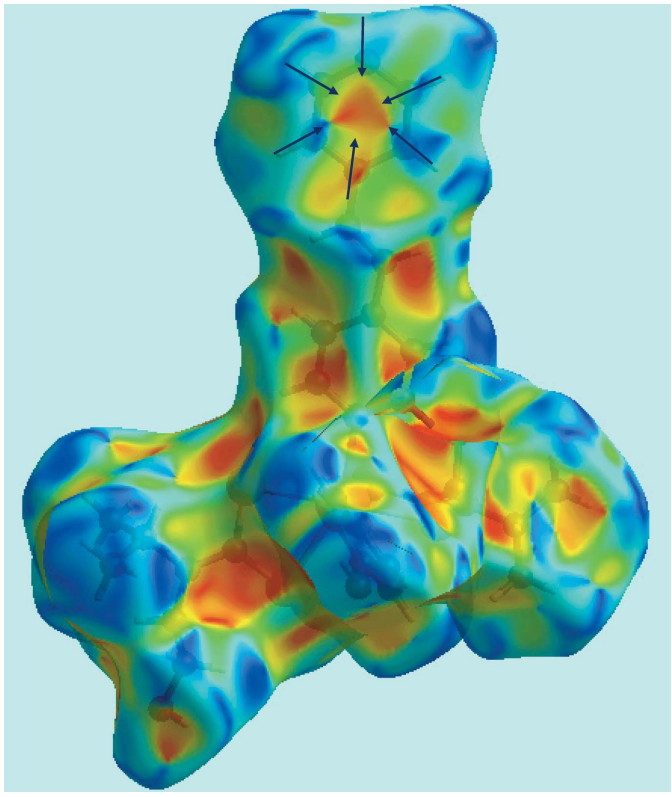

Figure 7
View of Hirshfeld surface mapped with shape-index property. The pairs of red and blue regions, identified with arrows, indicate π–π stacking interactions.

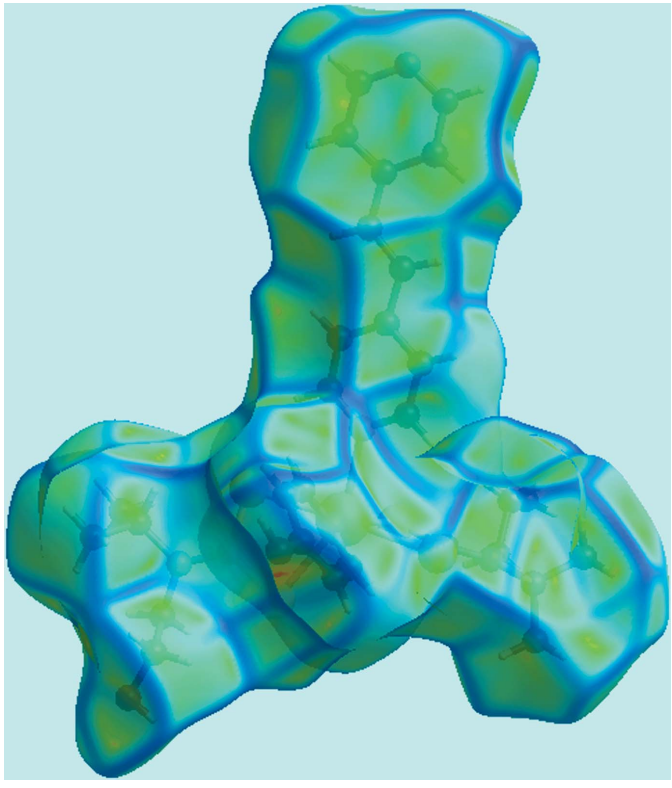

Figure 8
A view of Hirshfeld surface mapped over curvedness for (I). The flat regions highlight the involvement of rings in π–π stacking interactions.

Table 5
Enrichment ratios (ER).

Contact	ER
H···H	0.97
O···H/H···O	1.36
N···H/H···N	1.20
C···C	2.23
S···H/H···S	1.19
C···H/H···C	0.92
C···S/S···C	0.58
C···N/N···C	0.49

actions within the three-dimensional architecture described in *Supramolecular features* appear as the two distinct distributions of points in Fig. 6*f*. The vertex at $d_e = d_i = 1.6$ Å in the approximately triangular distribution of points in the plot corresponds to short intermolecular C···C contacts. The presence of π–π stacking interactions between the centrosymmetrically related N5-pyridyl rings [inter-centroid distance = 3.674 (2) Å, symmetry code: $3 - x, 1 - y, 2 - z$] is reflected through the appearance of green points around $d_e = d_i \sim 1.8$ Å, the red and blue triangle pairs on the Hirshfeld surface mapped with shape-index property identified with arrows in the image of Fig. 7, and in the flat region on the Hirshfeld surface mapped over curvedness in Fig. 8. Finally, the S···H/H···S contacts in the structure with a 10.3% contribution to the surface has a nearly symmetrical distribution of points, Fig. 6*g*, with the tips at $d_e + d_i \sim 2.95$ Å arising from the short interatomic S···H/H···S contacts listed in Table 3.

An additional descriptor, the enrichment ratio (ER), may be calculated on the basis of Hirshfeld surface analysis (Jelsch *et al.*, 2014). This provides further insight into the molecular packing as it indicates the relative propensities to form specific intermolecular interactions. The ER values for (I) are collected in Table 5. The ER value close to but slightly less than unity for H···H contacts, *i.e.* 0.97, is in accord with expectation (Jelsch *et al.*, 2014). The ER value of 1.36 for O···H/H···O contacts is in the expected 1.2–1.6 range and confirms the involvement of these atoms in the intermolecular O—H···O and C—H···O interactions. The ER value of 1.20 resulting from the 6% of the surface comprising nitrogen atoms and the 10.6% contribution to the Hirshfeld surface from N···H/H···N contacts is due to the presence of O—H···N hydrogen bonding and the C—H···N(acetonitrile) interaction. The high enrichment ratio of 2.23 for the C···C contacts reflects the formation of significant π–π stacking interactions and short C···C contacts as mentioned above. The ER value close to unity, *i.e.* 0.92, for C···H/H···C contacts shows their propensity to form short intermolecular C···H/H···C contacts. The ER values < 1 related to other contacts and low percentage contribution to the surface do not show any significance in the crystal packing.

5. Database survey

There is a sole example of a cadmium dithiocarbamate coordinated by bpe in the crystallographic literature (Groom *et al.*,

2016), namely $[Cd(S_2CNEt_2)_2(\mu\text{-bpe})]_n$, which is a linear coordination polymer with a *trans*-N_2S_4 donor set (Chai *et al.*, 2003). Reflecting the smaller size of zinc compared to cadmium, the zinc analogues are binuclear zero-dimensional with bpe bridging two five-coordinate (NS_4) zinc atoms (Arman *et al.*, 2009). Even in the presence of excess bpe, the $[Zn(S_2CNEt_2)_2]_2(\mu\text{-bpe})$ species still forms with non-coordinating bpe included in the structure (Lai & Tiekink, 2003). For the analogous xanthate structures, luminescent, zero-dimensional $[Zn(S_2COCyEt)_2]_2(\mu\text{-bpe})$ and one-dimensional $[Zn(S_2COEt)_2(\mu\text{-bpe})]_n$ are formed with the dimensionality correlated with the steric bulk of the xanthate-bound *R* groups (Kang *et al.*, 2010). With the sterically unencumbered cadmium dithiophosphate analogues, linear coordination polymers are formed regardless of the size of *R*, *i.e.* for $\{Cd[S_2P(OR)_2]_2(\mu\text{-bpe})\}_n$, *R* = *i*Pr and Cy (Lai & Tiekink, 2004).

There are literature precedents for both bidentate, bridging and monodentate bpe ligands in cadmium structures as observed in (I), *i.e.* $[Cd(NO_3)(\mu_2\text{-}NO_3)(\mu\text{-bpe})(bpe)(OH_2)]_n$ (Dong *et al.*, 1999) and $[Cd_2(SSO_3)_2(\mu\text{-bpe})(bpe)_2(OH_2)_4]_n$ (Paul *et al.*, 2011). Another structure has both bridging and monodentate bpe ligands as well as non-coordinating bpe ligands (and non-coordinating 4,4′-bipyridyl), *i.e.* $[Cd(NO_3)(\mu\text{-bpe})(bpe)_2(OH_2)_2]NO_3(bpe)(4,4'\text{-bipyridyl})(H_2O)_{4.45}$ (Lu *et al.*, 2001).

6. Synthesis and crystallization

The title compound was isolated regardless of the ratio, *i.e.* 2:1, 1:1 or 1:2, between the precursor molecules. In a typical experiment, $Cd[S_2CN(iPr)CH_2CH_2OH]_2$ (190 mg, 0.50 mmol) was dissolved in boiling acetonitrile (30 ml). *trans*-1,2-Dipyridin-4-ylethylene (47 mg, 0.25 mmol) was added to this solution, which was allowed to slowly cool to room temperature. Yellow prisms precipitated within an hour. The yield was not measured but was close to quantitative based on Cd. M.p. = 463–465 K (uncorrected). IR (neat solid, cm^{-1}): 1607 *m*, 1449 *ms*, 1407 *s*, 1170 *s*, 1037 *s*, 968 *s*, 954 *s*, 824 *s*. NMR: ^1H δ (p.p.m.): 8.6 (*dd*, Ar, 1.46 Hz, 4.68 Hz), 7.6 (*dd*, Ar, 1.46 Hz, 4.39 Hz), 7.54 (*s*, –CH═CH–), 5.21 (*sept*., –CH, 6.72 Hz), 4.82 (*t*, –OH, 5.56 Hz), 3.76-3.67 (*m*, $–CH_2–CH_2–$), 1.18 (*d*, CH_3, 6.72 Hz). TGA: one sharp step (onset at 497 K, mid-point at 502 K, end-point at 509 K; mass loss 62%) followed by a protracted mass loss totalling 71.5%, assigned to decomposition to CdS (calculated mass loss 69.5%).

7. Refinement

Crystal data, data collection and structure refinement details are summarized in Table 6. The carbon-bound H atoms were placed in calculated positions (C—H = 0.95–1.00 Å) and were included in the refinement in the riding-model approximation, with U_{iso}(H) set to 1.2–1.5U_{eq}(C). The oxygen-bound H atoms were located in a difference Fourier map but were refined with a distance restraint of O—H = 0.84±0.01 Å, and with U_{iso}(H) set to 1.5U_{eq}(O).

Table 6
Experimental details.

Crystal data	
Chemical formula	$[Cd_2(C_{12}H_{10}N_2)_3(C_6H_{12}NOS_2)_4]\cdot 4C_2H_3N$
M_r	1648.84
Crystal system, space group	Monoclinic, $P2_1/c$
Temperature (K)	153
a, *b*, *c* (Å)	16.884 (2), 14.4021 (15), 17.327 (2)
β (°)	109.112 (3)
V (Å^3)	3981.0 (8)
Z	2
Radiation type	Mo $K\alpha$
μ (mm^{-1})	0.80
Crystal size (mm)	0.35 × 0.25 × 0.10
Data collection	
Diffractometer	AFC12K/SATURN724
Absorption correction	Multi-scan (*ABSCOR*; Higashi, 1995)
T_{min}, T_{max}	0.752, 1.000
No. of measured, independent and observed [$I > 2\sigma(I)$] reflections	36088, 8240, 7736
R_{int}	0.033
(sin $\theta/\lambda)_{max}$ (Å^{-1})	0.628
Refinement	
$R[F^2 > 2\sigma(F^2)]$, $wR(F^2)$, *S*	0.047, 0.115, 1.13
No. of reflections	8240
No. of parameters	445
No. of restraints	2
$\Delta\rho_{max}$, $\Delta\rho_{min}$ (e Å^{-3})	1.43, −0.81

Computer programs: *CrystalClear* (Molecular Structure Corporation & Rigaku, 2005), *SHELXS97* (Sheldrick, 2008), *SHELXL2014* (Sheldrick, 2015), *ORTEP-3 for Windows* (Farrugia, 2012), *DIAMOND* (Brandenburg, 2006) and *publCIF* (Westrip, 2010).

References

Arman, H. D., Poplaukhin, P. & Tiekink, E. R. T. (2009). *Acta Cryst.* E**65**, m1472–m1473.
Brandenburg, K. (2006). *DIAMOND*. Crystal Impact GbR, Bonn, Germany.
Chai, J., Lai, C. S., Yan, J. & Tiekink, E. R. T. (2003). *Appl. Organomet. Chem.* **17**, 249–250.
Dong, Y. B., Layland, R. C., Smith, M. D., Pschirer, N. G., Bunz, U. H. F. & zur Loye, H.-C. (1999). *Inorg. Chem.* **38**, 3056–3060.
Farrugia, L. J. (2012). *J. Appl. Cryst.* **45**, 849–854.
Groom, C. R., Bruno, I. J., Lightfoot, M. P. & Ward, S. C. (2016). *Acta Cryst.* B**72**, 171–179.
Higashi, T. (1995). *ABSCOR*. Rigaku Corporation, Tokyo, Japan.
Howie, R. A., Tiekink, E. R. T., Wardell, J. L. & Wardell, S. M. S. V. (2009). *J. Chem. Crystallogr.* **39**, 293–298.
Jayatilaka, D., Grimwood, D. J., Lee, A., Lemay, A., Russel, A. J., Taylor, C., Wolff, S. K., Cassam-Chenai, P. & Whitton, A. (2005). *TONTO – A System for Computational Chemistry*. Available at: http://hirshfeldsurface.net/
Jelsch, C., Ejsmont, K. & Huder, L. (2014). *IUCrJ*, **1**, 119–128.
Jotani, M. M., Tan, Y. S. & Tiekink, E. R. T. (2016). *Z. Kristallogr.* **231**. doi: 10.1515/zkri-2016-1943.
Kang, J.-G., Shin, J.-S., Cho, D.-H., Jeong, Y.-K., Park, C., Soh, S. F., Lai, C. S. & Tiekink, E. R. T. (2010). *Cryst. Growth Des.* **10**, 1247–1256.
Lai, C. S. & Tiekink, E. R. T. (2003). *Appl. Organomet. Chem.* **17**, 251–252.
Lai, C. S. & Tiekink, E. R. T. (2004). *CrystEngComm*, **6**, 593–605.
Lu, J. Y., Runnels, K. A. & Norman, C. (2001). *Inorg. Chem.* **40**, 4516–4517.

McKinnon, J. J., Jayatilaka, D. & Spackman, M. A. (2007). *Chem Commun*. pp. 3814–3816.
McKinnon, J. J., Spackman, M. A. & Mitchell, A. S. (2004). *Acta Cryst.* B**60**, 627–668.
Molecular Structure Corporation & Rigaku (2005). *CrystalClear*. MSC, The Woodlands, Texas, USA, and Rigaku Corporation, Tokyo, Japan.
Paul, A. K., Karthik, R. & Natarajan, S. (2011). *Cryst. Growth Des.* **11**, 5741–5749.
Poplaukhin, P. & Tiekink, E. R. T. (2008). *Acta Cryst.* E**64**, m1176.
Rodina, T. A., Ivanov, A. V., Gerasimenko, A. V., Ivanov, M. A., Zaeva, A. S., Philippova, T. S. & Antzutkin, O. N. (2011). *Inorg. Chim. Acta*, **368**, 263–270.
Safbri, S. A. M., Halim, S. N. A., Jotani, M. M. & Tiekink, E. R. T. (2016). *Acta Cryst.* E**72**, 158–163.
Sheldrick, G. M. (2008). *Acta Cryst.* A**64**, 112–122.
Sheldrick, G. M. (2015). *Acta Cryst.* C**71**, 3–8.
Spackman, M. A., McKinnon, J. J. & Jayatilaka, D. (2008). *CrystEngComm*, **10**, 377–388.
Spek, A. L. (2009). *Acta Cryst.* D**65**, 148–155.
Tan, Y. S., Halim, S. N. A. & Tiekink, E. R. T. (2016). *Z. Kristallogr.* **231**, 113–126.
Tan, Y. S., Sudlow, A. L., Molloy, K. C., Morishima, Y., Fujisawa, K., Jackson, W. J., Henderson, W., Halim, S. N. B. A., Ng, S. W. & Tiekink, E. R. T. (2013). *Cryst. Growth Des*. **13**, 3046–3056.
Tiekink, E. R. T. (2003). *CrystEngComm*, **5**, 101–113.
Tiekink, E. R. T. & Zukerman-Schpector, J. (2011). *Chem. Commun.* **47**, 6623–6625.
Wahab, N. A. A., Baba, I., Mohamed Tahir, M. I. & Tiekink, E. R. T. (2011). *Acta Cryst.* E**67**, m551–m552.
Westrip, S. P. (2010). *J. Appl. Cryst.* **43**, 920–925.
Wolff, S. K., Grimwood, D. J., McKinnon, J. J., Turner, M. J., Jayatilaka, D. & Spackman, M. A. (2012). *Crystal Explorer*. The University of Western Australia.

supporting information

Acta Cryst. (2016). E**72**, 1085-1092 [https://doi.org/10.1107/S2056989016010768]

[μ_2-*trans*-1,2-Bis(pyridin-4-yl)ethene-κ^2N:N']bis{[1,2-bis(pyridin-4-yl)ethene-κN]bis[*N*-(2-hydroxyethyl)-*N*-isopropyldithiocarbamato-κ^2S,S']cadmium} acetonitrile tetrasolvate: crystal structure and Hirshfeld surface analysis

Mukesh M. Jotani, Pavel Poplaukhin, Hadi D. Arman and Edward R. T. Tiekink

Computing details

Data collection: *CrystalClear* (Molecular Structure Corporation & Rigaku, 2005); cell refinement: *CrystalClear* (Molecular Structure Corporation & Rigaku, 2005); data reduction: *CrystalClear* (Molecular Structure Corporation & Rigaku, 2005); program(s) used to solve structure: *SHELXS97* (Sheldrick, 2008); program(s) used to refine structure: *SHELXL2014* (Sheldrick, 2015); molecular graphics: *ORTEP-3 for Windows* (Farrugia, 2012) and *DIAMOND* (Brandenburg, 2006); software used to prepare material for publication: *publCIF* (Westrip, 2010).

[μ_2-*trans*-1,2-Bis(pyridin-4-yl)ethene-κ^2N:N']bis{[1,2-bis(pyridin-4-yl)ethene-κN]bis[*N*-(2-hydroxyethyl)-*N*-*N*-isopropyldithiocarbamato-κ^2S,S']cadmium} acetonitrile tetrasolvate:

Crystal data

$[Cd_2(C_{12}H_{10}N_2)_3(C_6H_{12}NOS_2)_4]\cdot 4C_2H_3N$
M_r = 1648.84
Monoclinic, $P2_1/c$
a = 16.884 (2) Å
b = 14.4021 (15) Å
c = 17.327 (2) Å
β = 109.112 (3)°
V = 3981.0 (8) Å^3
Z = 2
$F(000)$ = 1704
D_x = 1.376 Mg m^{-3}
Mo $K\alpha$ radiation, λ = 0.71073 Å
Cell parameters from 15613 reflections
θ = 2.5–30.5°
μ = 0.80 mm^{-1}
T = 153 K
Prism, yellow
0.35 × 0.25 × 0.10 mm

Data collection

AFC12K/SATURN724 diffractometer
Radiation source: fine-focus sealed tube
Graphite monochromator
ω scans
Absorption correction: multi-scan (ABSCOR; Higashi, 1995)
T_{min} = 0.752, T_{max} = 1.000
36088 measured reflections
8240 independent reflections
7736 reflections with $I > 2\sigma(I)$
R_{int} = 0.033
θ_{max} = 26.5°, θ_{min} = 2.0°
h = −21→19
k = −18→18
l = −21→21

Refinement

Refinement on F^2
Least-squares matrix: full
$R[F^2 > 2\sigma(F^2)]$ = 0.047
$wR(F^2)$ = 0.115
S = 1.13
8240 reflections
445 parameters
2 restraints
Hydrogen site location: mixed

$w = 1/[\sigma^2(F_o^2) + (0.0538P)^2 + 4.1818P]$
where $P = (F_o^2 + 2F_c^2)/3$
$(\Delta/\sigma)_{max} = 0.002$

$\Delta\rho_{max} = 1.43$ e Å^{-3}
$\Delta\rho_{min} = -0.81$ e Å^{-3}

Special details

Geometry. All esds (except the esd in the dihedral angle between two l.s. planes) are estimated using the full covariance matrix. The cell esds are taken into account individually in the estimation of esds in distances, angles and torsion angles; correlations between esds in cell parameters are only used when they are defined by crystal symmetry. An approximate (isotropic) treatment of cell esds is used for estimating esds involving l.s. planes.

Fractional atomic coordinates and isotropic or equivalent isotropic displacement parameters (Å²)

	x	*y*	*z*	U_{iso}*/U_{eq}
Cd	0.86121 (2)	0.27028 (2)	0.77182 (2)	0.02811 (9)
S1	0.91301 (5)	0.14219 (6)	0.88291 (5)	0.0409 (2)
S2	0.74876 (5)	0.12713 (5)	0.75128 (4)	0.03067 (16)
S3	0.80475 (5)	0.39522 (5)	0.65839 (5)	0.03553 (18)
S4	0.77645 (5)	0.40603 (5)	0.81826 (4)	0.03206 (17)
O1	0.65163 (14)	−0.17072 (16)	0.73753 (15)	0.0409 (6)
H1O	0.6124 (19)	−0.142 (3)	0.704 (2)	0.061*
O2	0.70145 (16)	0.70048 (15)	0.85595 (14)	0.0390 (5)
H2O	0.677 (3)	0.738 (2)	0.8189 (19)	0.059*
N1	0.81603 (16)	−0.00780 (17)	0.85909 (15)	0.0320 (5)
N2	0.71824 (16)	0.53113 (17)	0.69907 (15)	0.0315 (5)
N3	0.92734 (16)	0.19783 (18)	0.68118 (16)	0.0338 (6)
N4	1.00214 (16)	0.33683 (17)	0.82938 (15)	0.0309 (5)
N5	1.53044 (18)	0.5788 (2)	1.12686 (18)	0.0427 (7)
N6	0.4531 (4)	0.6223 (6)	0.6589 (4)	0.144 (3)
N7	0.4216 (5)	0.7244 (4)	0.4145 (4)	0.121 (2)
C1	0.82450 (19)	0.07842 (19)	0.83301 (18)	0.0295 (6)
C2	0.7352 (2)	−0.0575 (2)	0.82882 (19)	0.0352 (7)
H2A	0.6892	−0.0117	0.8191	0.042*
H2B	0.7311	−0.1006	0.8719	0.042*
C3	0.7226 (2)	−0.1119 (2)	0.7513 (2)	0.0373 (7)
H3A	0.7136	−0.0688	0.7047	0.045*
H3B	0.7730	−0.1497	0.7564	0.045*
C4	0.8842 (2)	−0.0533 (2)	0.92667 (19)	0.0345 (7)
H4	0.9366	−0.0166	0.9349	0.041*
C5	0.9014 (2)	−0.1517 (2)	0.9049 (2)	0.0408 (7)
H5A	0.9520	−0.1753	0.9465	0.061*
H5B	0.9097	−0.1518	0.8515	0.061*
H5C	0.8537	−0.1915	0.9028	0.061*
C6	0.8641 (3)	−0.0487 (3)	1.0054 (2)	0.0517 (9)
H6A	0.9121	−0.0716	1.0504	0.078*
H6B	0.8149	−0.0872	1.0006	0.078*
H6C	0.8524	0.0158	1.0162	0.078*
C7	0.76189 (18)	0.45215 (19)	0.72260 (18)	0.0283 (6)
C8	0.6803 (2)	0.5800 (2)	0.75284 (19)	0.0338 (7)
H8A	0.6565	0.5338	0.7814	0.041*

H8B	0.6337	0.6194	0.7191	0.041*
C9	0.7430 (2)	0.6407 (2)	0.8161 (2)	0.0361 (7)
H9A	0.7831	0.6006	0.8571	0.043*
H9B	0.7752	0.6784	0.7889	0.043*
C10	0.6999 (2)	0.5689 (2)	0.6145 (2)	0.0426 (8)
H10	0.7369	0.5350	0.5892	0.051*
C11	0.7209 (3)	0.6707 (3)	0.6145 (3)	0.0628 (11)
H11A	0.7093	0.6920	0.5581	0.094*
H11B	0.7803	0.6801	0.6453	0.094*
H11C	0.6866	0.7062	0.6401	0.094*
C12	0.6102 (3)	0.5471 (4)	0.5636 (2)	0.0681 (12)
H12A	0.5997	0.5692	0.5076	0.102*
H12B	0.5719	0.5782	0.5872	0.102*
H12C	0.6012	0.4799	0.5630	0.102*
C13	0.8862 (2)	0.1867 (2)	0.6011 (2)	0.0416 (8)
H13	0.8344	0.2182	0.5779	0.050*
C14	0.9149 (2)	0.1318 (2)	0.5505 (2)	0.0409 (8)
H14	0.8836	0.1268	0.4941	0.049*
C15	0.9902 (2)	0.0840 (2)	0.58273 (19)	0.0338 (7)
C16	1.0352 (2)	0.0992 (2)	0.6648 (2)	0.0351 (7)
H16	1.0886	0.0712	0.6888	0.042*
C17	1.0018 (2)	0.1548 (2)	0.7110 (2)	0.0359 (7)
H17	1.0331	0.1633	0.7671	0.043*
C18	1.0222 (2)	0.0174 (2)	0.53632 (19)	0.0355 (7)
H18	1.0787	−0.0024	0.5596	0.043*
C19	1.0297 (2)	0.4016 (2)	0.78886 (19)	0.0331 (6)
H19	0.9938	0.4200	0.7364	0.040*
C20	1.10796 (19)	0.4431 (2)	0.81939 (19)	0.0338 (6)
H20	1.1244	0.4887	0.7881	0.041*
C21	1.16227 (19)	0.4178 (2)	0.89581 (18)	0.0304 (6)
C22	1.13422 (19)	0.3486 (2)	0.93706 (18)	0.0334 (6)
H22	1.1696	0.3271	0.9887	0.040*
C23	1.0553 (2)	0.3117 (2)	0.90285 (18)	0.0337 (6)
H23	1.0374	0.2658	0.9329	0.040*
C24	1.2428 (2)	0.4655 (2)	0.93038 (19)	0.0337 (6)
H24	1.2517	0.5206	0.9042	0.040*
C25	1.3045 (2)	0.4366 (2)	0.99626 (19)	0.0356 (7)
H25	1.2965	0.3788	1.0190	0.043*
C26	1.38345 (19)	0.4854 (2)	1.03704 (19)	0.0339 (6)
C27	1.4043 (2)	0.5708 (2)	1.0115 (2)	0.0392 (7)
H27	1.3686	0.5987	0.9629	0.047*
C28	1.4775 (2)	0.6149 (3)	1.0576 (2)	0.0440 (8)
H28	1.4908	0.6732	1.0394	0.053*
C29	1.5114 (2)	0.4955 (3)	1.1492 (2)	0.0430 (8)
H29	1.5492	0.4681	1.1970	0.052*
C30	1.4403 (2)	0.4469 (2)	1.1072 (2)	0.0383 (7)
H30	1.4299	0.3875	1.1258	0.046*
C31	0.3930 (3)	0.6527 (4)	0.6166 (3)	0.0811 (16)

C32	0.3169 (3)	0.6944 (4)	0.5636 (3)	0.0715 (13)
H32A	0.3086	0.7549	0.5857	0.107*
H32B	0.2692	0.6539	0.5603	0.107*
H32C	0.3210	0.7027	0.5090	0.107*
C33	0.4380 (4)	0.6986 (4)	0.3603 (3)	0.0757 (14)
C34	0.4564 (4)	0.6632 (6)	0.2899 (4)	0.119 (3)
H34A	0.4786	0.5999	0.3012	0.178*
H34B	0.4980	0.7031	0.2782	0.178*
H34C	0.4049	0.6624	0.2426	0.178*

Atomic displacement parameters (Å²)

	U^{11}	U^{22}	U^{33}	U^{12}	U^{13}	U^{23}
Cd	0.02812 (14)	0.02260 (13)	0.03125 (13)	0.00156 (7)	0.00653 (10)	0.00010 (8)
S1	0.0366 (4)	0.0298 (4)	0.0430 (4)	−0.0089 (3)	−0.0052 (4)	0.0069 (3)
S2	0.0283 (4)	0.0252 (3)	0.0334 (4)	0.0014 (3)	0.0032 (3)	0.0011 (3)
S3	0.0419 (5)	0.0318 (4)	0.0335 (4)	0.0103 (3)	0.0132 (3)	0.0037 (3)
S4	0.0373 (4)	0.0265 (3)	0.0312 (4)	0.0030 (3)	0.0096 (3)	0.0016 (3)
O1	0.0307 (12)	0.0283 (11)	0.0510 (14)	−0.0040 (9)	−0.0041 (10)	0.0085 (10)
O2	0.0532 (15)	0.0263 (11)	0.0402 (12)	0.0070 (10)	0.0189 (11)	0.0020 (9)
N1	0.0309 (14)	0.0261 (12)	0.0331 (12)	−0.0038 (10)	0.0025 (11)	0.0019 (10)
N2	0.0324 (14)	0.0270 (12)	0.0335 (12)	0.0059 (10)	0.0086 (11)	0.0034 (10)
N3	0.0322 (14)	0.0327 (13)	0.0352 (13)	0.0048 (11)	0.0094 (11)	−0.0044 (11)
N4	0.0306 (13)	0.0261 (12)	0.0353 (13)	−0.0009 (10)	0.0096 (11)	−0.0012 (10)
N5	0.0317 (15)	0.0477 (16)	0.0436 (15)	−0.0062 (12)	0.0053 (12)	−0.0076 (13)
N6	0.081 (4)	0.252 (8)	0.111 (4)	0.064 (5)	0.049 (3)	0.090 (5)
N7	0.174 (7)	0.100 (4)	0.112 (4)	−0.036 (4)	0.076 (5)	−0.044 (3)
C1	0.0322 (16)	0.0232 (13)	0.0315 (14)	−0.0017 (11)	0.0084 (12)	−0.0016 (11)
C2	0.0311 (16)	0.0319 (15)	0.0394 (16)	−0.0069 (12)	0.0071 (13)	0.0028 (13)
C3	0.0311 (17)	0.0302 (15)	0.0445 (17)	−0.0047 (13)	0.0041 (14)	0.0037 (13)
C4	0.0309 (16)	0.0303 (15)	0.0366 (16)	0.0001 (12)	0.0034 (13)	0.0032 (13)
C5	0.046 (2)	0.0329 (16)	0.0393 (16)	0.0094 (14)	0.0086 (15)	0.0055 (14)
C6	0.055 (2)	0.060 (2)	0.0389 (17)	0.0110 (19)	0.0140 (17)	0.0000 (17)
C7	0.0239 (14)	0.0227 (13)	0.0340 (14)	−0.0010 (11)	0.0035 (12)	−0.0015 (11)
C8	0.0347 (17)	0.0265 (14)	0.0404 (16)	0.0058 (12)	0.0125 (14)	0.0007 (13)
C9	0.0349 (17)	0.0283 (15)	0.0435 (17)	0.0034 (13)	0.0110 (14)	−0.0024 (13)
C10	0.052 (2)	0.0368 (17)	0.0389 (17)	0.0166 (15)	0.0155 (16)	0.0121 (14)
C11	0.091 (3)	0.044 (2)	0.061 (2)	0.011 (2)	0.035 (2)	0.0156 (19)
C12	0.065 (3)	0.083 (3)	0.043 (2)	0.010 (2)	−0.001 (2)	0.007 (2)
C13	0.044 (2)	0.0375 (17)	0.0379 (16)	0.0130 (15)	0.0069 (15)	−0.0028 (14)
C14	0.048 (2)	0.0373 (17)	0.0332 (16)	0.0086 (15)	0.0073 (15)	−0.0029 (13)
C15	0.0381 (17)	0.0267 (14)	0.0390 (16)	0.0030 (12)	0.0157 (14)	0.0035 (13)
C16	0.0289 (16)	0.0320 (15)	0.0438 (17)	0.0026 (12)	0.0111 (14)	−0.0023 (13)
C17	0.0317 (16)	0.0345 (16)	0.0381 (16)	0.0011 (13)	0.0068 (13)	−0.0055 (13)
C18	0.0372 (17)	0.0322 (15)	0.0394 (15)	0.0036 (13)	0.0156 (14)	0.0050 (13)
C19	0.0329 (16)	0.0317 (15)	0.0321 (14)	−0.0006 (12)	0.0072 (13)	0.0017 (12)
C20	0.0324 (16)	0.0313 (15)	0.0367 (15)	−0.0019 (12)	0.0102 (13)	0.0044 (13)
C21	0.0267 (15)	0.0291 (14)	0.0338 (14)	−0.0027 (11)	0.0077 (12)	−0.0039 (12)

C22	0.0300 (16)	0.0342 (15)	0.0311 (14)	−0.0032 (12)	0.0032 (12)	−0.0005 (12)
C23	0.0340 (17)	0.0317 (15)	0.0321 (15)	−0.0030 (12)	0.0066 (13)	0.0032 (12)
C24	0.0340 (17)	0.0304 (15)	0.0369 (15)	−0.0042 (12)	0.0119 (13)	0.0000 (13)
C25	0.0335 (17)	0.0361 (16)	0.0356 (15)	−0.0045 (13)	0.0093 (13)	−0.0001 (13)
C26	0.0298 (16)	0.0357 (15)	0.0360 (15)	−0.0051 (12)	0.0106 (13)	−0.0049 (13)
C27	0.0317 (17)	0.0404 (17)	0.0398 (17)	−0.0012 (14)	0.0039 (14)	0.0015 (14)
C28	0.0363 (19)	0.0414 (18)	0.0506 (19)	−0.0076 (14)	0.0090 (16)	−0.0005 (16)
C29	0.0334 (18)	0.056 (2)	0.0350 (16)	−0.0043 (15)	0.0050 (14)	0.0002 (15)
C30	0.0328 (17)	0.0418 (18)	0.0392 (16)	−0.0061 (14)	0.0106 (14)	0.0020 (14)
C31	0.065 (3)	0.119 (5)	0.070 (3)	0.016 (3)	0.037 (3)	0.033 (3)
C32	0.057 (3)	0.093 (4)	0.060 (3)	−0.002 (3)	0.014 (2)	0.014 (3)
C33	0.084 (4)	0.068 (3)	0.076 (3)	−0.018 (3)	0.028 (3)	−0.015 (3)
C34	0.087 (4)	0.193 (8)	0.085 (4)	−0.049 (5)	0.040 (3)	−0.059 (5)

Geometric parameters (Å, º)

Cd—S1	2.6019 (8)	C10—C12	1.514 (6)
Cd—S2	2.7457 (8)	C10—H10	1.0000
Cd—S3	2.6043 (8)	C11—H11A	0.9800
Cd—S4	2.6967 (8)	C11—H11B	0.9800
Cd—N3	2.439 (3)	C11—H11C	0.9800
Cd—N4	2.454 (3)	C12—H12A	0.9800
C1—S1	1.726 (3)	C12—H12B	0.9800
C1—S2	1.717 (3)	C12—H12C	0.9800
C7—S3	1.721 (3)	C13—C14	1.381 (5)
C7—S4	1.727 (3)	C13—H13	0.9500
O1—C3	1.422 (4)	C14—C15	1.391 (5)
O1—H1O	0.839 (10)	C14—H14	0.9500
O2—C9	1.425 (4)	C15—C16	1.393 (4)
O2—H2O	0.840 (10)	C15—C18	1.464 (4)
N1—C1	1.345 (4)	C16—C17	1.377 (4)
N1—C2	1.477 (4)	C16—H16	0.9500
N1—C4	1.498 (4)	C17—H17	0.9500
N2—C7	1.344 (4)	C18—C18^{i}	1.334 (6)
N2—C8	1.472 (4)	C18—H18	0.9500
N2—C10	1.497 (4)	C19—C20	1.388 (4)
N3—C17	1.343 (4)	C19—H19	0.9500
N3—C13	1.343 (4)	C20—C21	1.390 (4)
N4—C19	1.339 (4)	C20—H20	0.9500
N4—C23	1.345 (4)	C21—C22	1.396 (4)
N5—C29	1.333 (5)	C21—C24	1.465 (4)
N5—C28	1.344 (5)	C22—C23	1.375 (4)
N6—C31	1.128 (7)	C22—H22	0.9500
N7—C33	1.126 (7)	C23—H23	0.9500
C2—C3	1.508 (5)	C24—C25	1.335 (4)
C2—H2A	0.9900	C24—H24	0.9500
C2—H2B	0.9900	C25—C26	1.468 (4)
C3—H3A	0.9900	C25—H25	0.9500

C3—H3B	0.9900	C26—C27	1.391 (5)
C4—C6	1.510 (5)	C26—C30	1.393 (5)
C4—C5	1.519 (4)	C27—C28	1.386 (5)
C4—H4	1.0000	C27—H27	0.9500
C5—H5A	0.9800	C28—H28	0.9500
C5—H5B	0.9800	C29—C30	1.375 (5)
C5—H5C	0.9800	C29—H29	0.9500
C6—H6A	0.9800	C30—H30	0.9500
C6—H6B	0.9800	C31—C32	1.443 (7)
C6—H6C	0.9800	C32—H32A	0.9800
C8—C9	1.525 (4)	C32—H32B	0.9800
C8—H8A	0.9900	C32—H32C	0.9800
C8—H8B	0.9900	C33—C34	1.445 (8)
C9—H9A	0.9900	C34—H34A	0.9800
C9—H9B	0.9900	C34—H34B	0.9800
C10—C11	1.510 (5)	C34—H34C	0.9800

S1—Cd—S2	67.31 (2)	C11—C10—C12	113.0 (3)
S1—Cd—S3	178.06 (3)	N2—C10—H10	107.0
S1—Cd—S4	112.08 (3)	C11—C10—H10	107.0
S1—Cd—N3	93.39 (7)	C12—C10—H10	107.0
S1—Cd—N4	85.98 (6)	C10—C11—H11A	109.5
S2—Cd—S3	110.75 (3)	C10—C11—H11B	109.5
S2—Cd—S4	99.85 (3)	H11A—C11—H11B	109.5
S2—Cd—N3	92.19 (7)	C10—C11—H11C	109.5
S2—Cd—N4	152.04 (6)	H11A—C11—H11C	109.5
S3—Cd—S4	68.00 (2)	H11B—C11—H11C	109.5
S3—Cd—N3	86.63 (7)	C10—C12—H12A	109.5
S3—Cd—N4	95.94 (6)	C10—C12—H12B	109.5
S4—Cd—N3	154.39 (6)	H12A—C12—H12B	109.5
S4—Cd—N4	97.72 (6)	C10—C12—H12C	109.5
N3—Cd—N4	80.87 (9)	H12A—C12—H12C	109.5
C1—S1—Cd	88.88 (10)	H12B—C12—H12C	109.5
C1—S2—Cd	84.44 (10)	N3—C13—C14	123.6 (3)
C7—S3—Cd	88.21 (10)	N3—C13—H13	118.2
C7—S4—Cd	85.13 (10)	C14—C13—H13	118.2
C3—O1—H1O	104 (3)	C13—C14—C15	119.5 (3)
C9—O2—H2O	102 (3)	C13—C14—H14	120.2
C1—N1—C2	121.0 (3)	C15—C14—H14	120.2
C1—N1—C4	121.8 (2)	C14—C15—C16	117.0 (3)
C2—N1—C4	116.8 (2)	C14—C15—C18	123.8 (3)
C7—N2—C8	121.5 (3)	C16—C15—C18	119.2 (3)
C7—N2—C10	121.4 (3)	C17—C16—C15	119.6 (3)
C8—N2—C10	116.9 (2)	C17—C16—H16	120.2
C17—N3—C13	116.4 (3)	C15—C16—H16	120.2
C17—N3—Cd	121.2 (2)	N3—C17—C16	123.7 (3)
C13—N3—Cd	121.7 (2)	N3—C17—H17	118.2
C19—N4—C23	116.4 (3)	C16—C17—H17	118.2

C19—N4—Cd	121.1 (2)	C18^{i}—C18—C15	124.8 (4)
C23—N4—Cd	122.5 (2)	C18^{i}—C18—H18	117.6
C29—N5—C28	117.0 (3)	C15—C18—H18	117.6
N1—C1—S2	121.5 (2)	N4—C19—C20	123.4 (3)
N1—C1—S1	119.5 (2)	N4—C19—H19	118.3
S2—C1—S1	119.00 (17)	C20—C19—H19	118.3
N1—C2—C3	114.3 (3)	C19—C20—C21	119.9 (3)
N1—C2—H2A	108.7	C19—C20—H20	120.0
C3—C2—H2A	108.7	C21—C20—H20	120.0
N1—C2—H2B	108.7	C20—C21—C22	116.5 (3)
C3—C2—H2B	108.7	C20—C21—C24	120.1 (3)
H2A—C2—H2B	107.6	C22—C21—C24	123.4 (3)
O1—C3—C2	109.0 (3)	C23—C22—C21	119.9 (3)
O1—C3—H3A	109.9	C23—C22—H22	120.1
C2—C3—H3A	109.9	C21—C22—H22	120.1
O1—C3—H3B	109.9	N4—C23—C22	123.8 (3)
C2—C3—H3B	109.9	N4—C23—H23	118.1
H3A—C3—H3B	108.3	C22—C23—H23	118.1
N1—C4—C6	110.1 (3)	C25—C24—C21	124.3 (3)
N1—C4—C5	112.0 (3)	C25—C24—H24	117.8
C6—C4—C5	112.5 (3)	C21—C24—H24	117.8
N1—C4—H4	107.3	C24—C25—C26	126.5 (3)
C6—C4—H4	107.3	C24—C25—H25	116.8
C5—C4—H4	107.3	C26—C25—H25	116.8
C4—C5—H5A	109.5	C27—C26—C30	117.2 (3)
C4—C5—H5B	109.5	C27—C26—C25	123.7 (3)
H5A—C5—H5B	109.5	C30—C26—C25	119.1 (3)
C4—C5—H5C	109.5	C28—C27—C26	119.5 (3)
H5A—C5—H5C	109.5	C28—C27—H27	120.3
H5B—C5—H5C	109.5	C26—C27—H27	120.3
C4—C6—H6A	109.5	N5—C28—C27	123.0 (3)
C4—C6—H6B	109.5	N5—C28—H28	118.5
H6A—C6—H6B	109.5	C27—C28—H28	118.5
C4—C6—H6C	109.5	N5—C29—C30	123.8 (3)
H6A—C6—H6C	109.5	N5—C29—H29	118.1
H6B—C6—H6C	109.5	C30—C29—H29	118.1
N2—C7—S3	120.8 (2)	C29—C30—C26	119.5 (3)
N2—C7—S4	120.5 (2)	C29—C30—H30	120.3
S3—C7—S4	118.65 (16)	C26—C30—H30	120.3
N2—C8—C9	112.6 (3)	N6—C31—C32	178.2 (9)
N2—C8—H8A	109.1	C31—C32—H32A	109.5
C9—C8—H8A	109.1	C31—C32—H32B	109.5
N2—C8—H8B	109.1	H32A—C32—H32B	109.5
C9—C8—H8B	109.1	C31—C32—H32C	109.5
H8A—C8—H8B	107.8	H32A—C32—H32C	109.5
O2—C9—C8	111.0 (3)	H32B—C32—H32C	109.5
O2—C9—H9A	109.4	N7—C33—C34	177.8 (7)
C8—C9—H9A	109.4	C33—C34—H34A	109.5

O2—C9—H9B	109.4	C33—C34—H34B	109.5
C8—C9—H9B	109.4	H34A—C34—H34B	109.5
H9A—C9—H9B	108.0	C33—C34—H34C	109.5
N2—C10—C11	112.3 (3)	H34A—C34—H34C	109.5
N2—C10—C12	110.1 (3)	H34B—C34—H34C	109.5
C2—N1—C1—S2	−11.5 (4)	C13—C14—C15—C16	−3.7 (5)
C4—N1—C1—S2	175.8 (2)	C13—C14—C15—C18	174.0 (3)
C2—N1—C1—S1	168.1 (2)	C14—C15—C16—C17	4.0 (5)
C4—N1—C1—S1	−4.6 (4)	C18—C15—C16—C17	−173.9 (3)
Cd—S2—C1—N1	−174.7 (3)	C13—N3—C17—C16	−2.1 (5)
Cd—S2—C1—S1	5.71 (16)	Cd—N3—C17—C16	168.2 (2)
Cd—S1—C1—N1	174.4 (2)	C15—C16—C17—N3	−1.1 (5)
Cd—S1—C1—S2	−6.00 (17)	C14—C15—C18—C18^{i}	−12.2 (6)
C1—N1—C2—C3	87.7 (4)	C16—C15—C18—C18^{i}	165.5 (4)
C4—N1—C2—C3	−99.3 (3)	C23—N4—C19—C20	−0.9 (4)
N1—C2—C3—O1	168.4 (2)	Cd—N4—C19—C20	178.4 (2)
C1—N1—C4—C6	101.6 (3)	N4—C19—C20—C21	0.1 (5)
C2—N1—C4—C6	−71.4 (4)	C19—C20—C21—C22	1.5 (4)
C1—N1—C4—C5	−132.3 (3)	C19—C20—C21—C24	−176.2 (3)
C2—N1—C4—C5	54.6 (4)	C20—C21—C22—C23	−2.2 (4)
C8—N2—C7—S3	179.2 (2)	C24—C21—C22—C23	175.4 (3)
C10—N2—C7—S3	4.5 (4)	C19—N4—C23—C22	0.1 (5)
C8—N2—C7—S4	−1.1 (4)	Cd—N4—C23—C22	−179.2 (2)
C10—N2—C7—S4	−175.8 (2)	C21—C22—C23—N4	1.5 (5)
Cd—S3—C7—N2	−179.5 (2)	C20—C21—C24—C25	−168.5 (3)
Cd—S3—C7—S4	0.81 (16)	C22—C21—C24—C25	13.9 (5)
Cd—S4—C7—N2	179.5 (2)	C21—C24—C25—C26	−174.9 (3)
Cd—S4—C7—S3	−0.78 (15)	C24—C25—C26—C27	0.4 (5)
C7—N2—C8—C9	81.4 (3)	C24—C25—C26—C30	177.9 (3)
C10—N2—C8—C9	−103.6 (3)	C30—C26—C27—C28	−2.4 (5)
N2—C8—C9—O2	168.5 (2)	C25—C26—C27—C28	175.1 (3)
C7—N2—C10—C11	−131.1 (3)	C29—N5—C28—C27	2.3 (5)
C8—N2—C10—C11	53.9 (4)	C26—C27—C28—N5	0.0 (5)
C7—N2—C10—C12	102.0 (4)	C28—N5—C29—C30	−2.2 (5)
C8—N2—C10—C12	−72.9 (4)	N5—C29—C30—C26	−0.2 (5)
C17—N3—C13—C14	2.4 (5)	C27—C26—C30—C29	2.5 (5)
Cd—N3—C13—C14	−167.9 (3)	C25—C26—C30—C29	−175.1 (3)
N3—C13—C14—C15	0.6 (6)		

Symmetry code: (i) −*x*+2, −*y*, −*z*+1.

Hydrogen-bond geometry (Å, º)

D—H···*A*	*D*—H	H···*A*	*D*···*A*	*D*—H···*A*
O1—H1*O*···N5^{ii}	0.83 (4)	1.82 (4)	2.655 (4)	177 (3)
O2—H2*O*···O1^{iii}	0.84 (3)	1.87 (3)	2.689 (3)	165 (5)

C25—H25···O2^{iv}	0.95	2.44	3.261 (4)	145
C28—H28···N7^{v}	0.95	2.56	3.296 (7)	134

Symmetry codes: (ii) $x-1, -y+1/2, z-1/2$; (iii) $x, y+1, z$; (iv) $-x+2, -y+1, -z+2$; (v) $x+1, -y+3/2, z+1/2$.